Published OnlineFirst July 23, 2012; DOI: 10.1158/1078-0432.CCR-12-0792

Cancer Therapy: Preclinical

Clinical Cancer Research

Targeting Stat3 Abrogates EGFR Inhibitor Resistance in Cancer

Malabika Sen[1], Sonali Joyce[1], Mary Panahandeh[1], Changyou Li[2], Sufi M. Thomas[1], Jessica Maxwell[1], Lin Wang[3], William E. Gooding[4], Daniel E. Johnson[2,5], and Jennifer R. Grandis[1,5]

Abstract

Purpose: EGF receptor (EGFR) is upregulated in most epithelial cancers where signaling through EGFR contributes to cancer cell proliferation and survival. The limited clinical efficacy of EGFR inhibitors suggests that identification of resistance mechanisms may identify new pathways for therapeutic targeting. STAT3 is upregulated in many cancers and activated via both EGFR-dependent and -independent pathways. In the present study, we tested the consequences of STAT3 inhibition in EGFR inhibitor–resistant head and neck squamous cell carcinoma (HNSCC) and bladder cancer models to determine whether STAT3 blockade can enhance responses to EGFR targeting.

Experimental Design: pSTAT3 expression was assessed in human HNSCC tumors that recurred following cetuximab treatment. Cetuximab-sensitive and -resistant cell lines were treated with a STAT3 decoy to determine EC_{50} concentrations and the effects on STAT3 target gene expression by Western blotting. *In vivo* assays included evaluation of antitumor efficacy of STAT3 decoy in cetuximab-sensitive and -resistant models followed by immunoblotting for STAT3 target protein expression.

Results: Targeting STAT3 with a STAT3 decoy reduced cellular viability and the expression of STAT3 target genes in EGFR inhibitor resistance models. The addition of a STAT3 inhibitor to EGFR blocking strategies significantly enhanced antitumor effects *in vivo*. Biopsies from HNSCC tumors that recurred following cetuximab treatment showed increased STAT3 activation compared with pretreatment biopsies.

Conclusions: These results suggest that STAT3 activation contributes to EGFR inhibitor resistance both in HNSCC and bladder cancer where concomitant targeting of STAT3 may represent an effective treatment strategy. *Clin Cancer Res; 18(18); 4986–96. ©2012 AACR.*

Introduction

EGF receptor (EGFR) is hyperactivated in multiple cancers and has emerged as a validated therapeutic target in several solid tumors (1). EGFR monoclonal antibodies such as cetuximab and panitumumab (Erbitux, Vectibix) are U.S. Food and Drug Administration (FDA)-approved for the treatment of advanced head and neck squamous cell carcinoma (HNSCC) and/or colorectal cancer in combination with either radiotherapy or chemotherapy. The EGFR-selective tyrosine kinase inhibitor (TKI) erlotinib (Tarceva) is approved for the treatment of non–small cell lung cancer (NSCLC) and pancreatic cancer, although profound efficacy is generally limited to NSCLC tumors harboring EGFR activating mutations (2–8). The paucity of EGFR inhibitor resistance models and the limited availability of tumor biopsies in the setting of EGFR inhibitor resistance have contributed to an incomplete understanding of the mechanisms that contribute to intrinsic or acquired resistance to EGFR targeting in some cancers. Elucidation of EGFR inhibitor resistance mechanisms may identify pathways that can be targeted to enhance treatment responses.

Overactivation of multiple signaling pathways contributes to EGFR inhibitor resistance as cancers of different origins use different mechanisms to escape EGFR therapy. In erlotinib-resistant lung cancer cells, increased expression of interleukin-6 (IL-6) has been shown to be responsible for the EGFR-independent STAT3 phosphorylation (9). Overactivation of VEGF has been shown to play a role in resistance to anti-EGFR therapy and combined blockade of VEGF and EGFR pathways with DC101, an anti-VEGF receptor monoclonal antibody, and cetuximab, respectively, have shown greater inhibition of tumor growth than single agent in both gastric and colon cancer (10). Overexpression of HER-2, the second member of the erbB family, contributes to EGFR inhibitor resistance and targeting both EGFR and HER-2 using a dual tyrosine kinase inhibitor such as lapatinib showed activity in breast cancer cell lines overexpressing HER-2 (11).

Authors' Affiliations: Departments of [1]Otolaryngology, [2]Medicine, [3]Pathology, [4]Biostatistics, and [5]Pharmacology & Chemical Biology, University of Pittsburgh School of Medicine and University of Pittsburgh Cancer Institute, Pittsburgh, Pennsylvania

Corresponding Author: Jennifer R. Grandis, University of Pittsburgh School of Medicine, 200 Lothrop Street, Suite 500, Pittsburgh, PA 15213. Phone: 412-647-5979; Fax: 412-383-5409; E-mail: jgrandis@pitt.edu

doi: 10.1158/1078-0432.CCR-12-0792

Published OnlineFirst July 23, 2012; DOI: 10.1158/1078-0432.CCR-12-0792

Translational Relevance

Cumulative evidence suggests that STAT3 may contribute to therapeutic resistance, and targeting STAT3 represents a potential strategy to improve treatment responses. Although compounds that decrease STAT3 activation have been used to reduce therapeutic resistance, none of the agents selectively or specifically inhibit STAT3. In this study, human head and neck squamous cell carcinoma (HNSCC) that recurred following cetuximab treatment showed increased pSTAT3 expression. Treatment with a transcription factor decoy oligonucleotide specifically targeting STAT3 inhibited the growth of preclinical cancer models that were resistant to EGF receptor (EGFR) inhibitors. These findings suggest that targeting STAT3 may be effective in the setting of EGFR inhibitor resistance to augment treatment responses.

STAT3, a member of the STAT family of transcription factors, is activated in several cancers (12). STAT3 tyrosine phosphorylation can be induced by stimulation of upstream receptor and/or nonreceptor kinases including EGFR (13), IL-6/gp130 and Janus-activated kinases (JAK; ref. 14), and Src family kinases (15). STAT3 activation has been identified in the setting of resistance to EGFR tyrosine kinases inhibitors in preclinical models of glioma and HNSCCs (12, 16), and resistance to neoadjuvant EGFR TKI treatment of patients with NSCLCs was associated with elevated STAT3 activity in patient tumors (17). These cumulative results suggest that STAT3 may be activated in the setting of resistance to EGFR inhibitor therapy where targeting STAT3 may overcome either *de novo* or acquired resistance.

In the absence of a small molecule with STAT3-selective activity, we developed a transcription factor decoy oligonucleotide, which has been shown to block STAT3-mediated DNA binding and inhibit tumor cell proliferation *in vitro* and xenograft growth *in vivo* in a wide variety of preclinical cancer models including xenografts and transgenic models (18–25). Combined treatment of HNSCC cell lines with the STAT3 decoy and EGFR TKI was associated with enhanced antitumor effects (26). In the present study, we tested the antitumor effects of STAT3 inhibition using the STAT3 decoy in preclinical cancer models of intrinsic or acquired resistance to EGFR TKI or cetuximab in tumor models not characterized by activating EGFR mutations. Furthermore, assessment of pSTAT3 in human HNSCC tumors that recurred following cetuximab treatment showed increased pSTAT3 staining compared with levels in pretreatment biopsies. These findings suggest that targeting STAT3 may enhance the antitumor effects of EGFR inhibitors.

Materials and Methods

Cell line validation

The HNSCC cell lines Cal33, 686LN, HN5, and OSC19 and the bladder cancer cell line T24 were validated using the AmpFlSTR Profiler Plus Kit from PE Biosystems according to the manufacturer's instructions.

Cell culture

HNSCC cell lines Cal33 (a kind gift from Jean Louis Fischel, Centre Antoine Lacassagne), HN5, and OSC19 were cultured in Dulbecco's Modified Eagle's Medium (DMEM; Mediatech, Inc.) containing 10% heat-inactivated FBS at 37°C with 5% CO_2. 686 LN (a kind gift from Georgia Chen, University of Emory, Atlanta, GA) was maintained in DMEM/F12 media (1:1) from Gibco containing 10% heat-inactivated FBS (ISC BioExpress). The T24 bladder cancer cell line was obtained from American Type Culture Collection. The cetuximab-resistant cell lines, T24 PR1, T24 PR2, and T24 PR3, were generated *in vivo* by exposing tumor-bearing athymic nude mice generated from the parental cell line T24 to increasing concentrations of cetuximab over a 3-month period, as described previously (27). T24 cells were cultured in DMEM (Mediatech, Inc.) containing 10% heat-inactivated FBS. The cetuximab-resistant cell lines, T24 PR1, T24 PR2, and T24 PR3, were maintained in presence of cetuximab at a concentration of 100 nmol/L in DMEM containing 10% heat-inactivated FBS.

Immunohistochemical analysis and construction of tissue microarrays

Tumor biopsies were obtained from 7 patients with HNSCCs before cetuximab treatment and 15 patients following cetuximab treatment under a protocol approved by the Institutional Review Board at the University of Pittsburgh (Pittsburgh, PA; IRB#991206). Informed consent was obtained from all subjects. The average composite score (intensity of staining × the percentage of tumor cells that stained positively) of pre- and post–cetuximab-treated tumors are represented. Using a manual tissue array instrument (MTA-1; Beecher Instruments), a paraffin core of 1.0-mm was taken from a representative region of the donor block and arrayed into a blank recipient paraffin block in duplicate. The newly constructed array block was then warmed to 37°C for 10 minutes to allow annealing of donor cores to the paraffin wax of the recipient block while minimizing core loss. Donor cores ranged from 2 to 4 mm in length. Immunohistochemistry (IHC) was carried out on formalin-fixed, paraffin-embedded tissue microarray (TMA) sections by using antibodies against pSTAT3 (1:75 dilution, 1:75 overnight 4°C incubation, Santa Cruz Biotechnology). TMA sections were subjected to antigen retrieval for 15 minutes in 0.01 mol/L citrate buffer. TMAs were blocked and stained with primary antibodies. Following three 5-minute washes, TMAs were incubated with biotinylated anti-rabbit secondary antibody followed by treatment with avidin–biotin complex. Signal was developed with 3,3′-diaminobenzidine (DAB) substrate, modestly counterstained with hematoxylin, and slides were analyzed microscopically. Immunohistochemical staining was assessed semiquantitatively for each core. The percentage of immunoreactive cells was recorded and rounded to the nearest 10 percentile. Cytoplasmic staining was graded

Published OnlineFirst July 23, 2012; DOI: 10.1158/1078-0432.CCR-12-0792

for intensity (0, negative; 1, weak; 2, moderate; and 3, strong) A composite score was obtained by multiplying the intensity and the percentage staining score. The scores across replicate cores on slides were averaged. The average composite score for both antibodies were graphed by GraphPad Prism Software.

Reagents

Cetuximab (Erbitux) was purchased from the research pharmacy at the University of Pittsburgh Cancer Institute. Erlotinib (OSI-774; Tarceva) was purchased from North-West Pharmacy.

STAT3 decoy design and synthesis

The STAT3 decoy sequence was 5′-CATTTCCCGTAAATC-3′, 3′-GTAAAGGGCATTTAG-5′ and the mutant control decoy sequence, which differed by one nucleotide at position 9 (G to T), was 5′-CATTTCCCTTAAATC-3′, 3′-GTAA-AGGGAATTTAG-5′, as described previously (18). The single-stranded sense and antisense oligonucleotides were synthesized by Integrated DNA Technologies with phosphorothioate modifications of the residues on 3′ and 5′ ends, as previously described (18).

Dose–response experiments

HN5, OSC19, T24, and the TKI- and cetuximab-resistant cells (686LN, Cal33, T24 PR1, T24 PR2, and T24 PR3) were seeded in 24-well plates in DMEM containing FBS. After 24 hours, cells were transfected with increasing concentrations of STAT3 decoy (26). After 4 hours of transfection, media were replaced with DMEM containing 10% FBS. After 72 hours, MTT assays were conducted to determine percentage of cell viability. To determine the dose response of erlotinib in the parental (T24) and cetuximab-resistant bladder cancer cell lines (T24 PR1, T24 PR2, and T24 PR3) as well as the TKI-sensitive (HN5 and OSC19) and -resistant (686LN and Cal33) HNSCC cell lines, the cells were plated in 24-well plates in DMEM containing FBS. After 24 hours, cells were treated with varying concentrations of erlotinib in DMEM containing FBS. Dimethyl sulfoxide served as a vehicle control. After 72 hours, MTT assays were conducted to determine percentage of cell viability.

ELISA

Cetuximab-resistant (T24 PR1, T24 PR2 and T24 PR3) and -sensitive (T24) bladder cancer cells were plated, and after 24 hours, cells were cultured in serum-free medium, and 24 hours later, cells were collected and analyzed in duplicate with a human IL6 ELISA kit (R&D Systems). This experiment was repeated 3 times. Results are reported as means ± SD.

Immunoblotting

Cells were plated at a density of 8×10^5 cells/10-cm plate and after 24 hours transfected with the EC_{50} concentrations of STAT3 decoy for the respective cell lines. After 4 hours, the transfection media were replaced with DMEM + 10% FBS. After 24 hours, the cells were harvested, and protein content was determined using Bradford's reagent (BIO-RAD; ref. 26). Proteins (40 μg/lane) were separated by 10% SDS-PAGE, probed with rabbit anti-human cyclin D1 polyclonal antibody or mouse anti-human Bcl-X_L monoclonal antibody (Santa Cruz Biotechnology), and developed using the Enhanced Chemiluminescence (ECL) Detection System (Amersham Life Sciences Inc.). The membranes were stripped and re-probed with rabbit anti-human β-tubulin polyclonal antibody (Abcam Inc.), as a loading control. Densitometric analyses were conducted using ImageJ software.

In vivo tumor xenograft studies

(A) Female athymic nude mice *nu/nu* (4–6 weeks old; 20 g; Harlan Sprague–Dawley) were inoculated with T24 cells (2×10^6 cells) into the right and left flanks resulting in 2 tumors per mouse (9 mice per group). Similarly, another group of mice (8 mice per group) were inoculated with the C225-resistant cells T24 PR3 (2×10^6 cells) in both the flanks. Once the tumors were palpable, mice were treated with STAT3 decoy/STAT3 mutant and cetuximab. Intratumoral injection of the STAT3 decoy/STAT3 mutant (50 μg) was delivered daily. Cetuximab was injected intraperitoneally (i.p.) at a dose of 1 mg/mouse, 3 times a week. Mice were sacrificed after 20 days and tumors were harvested for analysis. Animal care was in strict compliance with institutional guidelines established by the University of Pittsburgh, the Guide for the Care and Use of Laboratory Animals (National Academy of Sciences, 1996), and the Association for Assessment and Accreditation of Laboratory Animal Care International. (B) Female athymic nude mice (10 mice) *nu/nu* (4–6 weeks old; 20 g; Harlan Sprague–Dawley) were inoculated with 686LN cells (1×10^6 cells) into the right and left flanks resulting in 2 tumors per mouse. Once the tumors were palpable, mice were treated with STAT3 decoy/STAT3 mutant and cetuximab. Intratumoral injection of the STAT3 decoy/STAT3 mutant (50 μg) was delivered daily. Cetuximab was injected i.p. at a dose of 0.2 mg/mouse, 2 times a week and the treatment was continued until day 20. Animal care was in strict compliance with institutional guidelines established by the University of Pittsburgh, the Guide for the Care and Use of Laboratory Animals (National Academy of Sciences, 1996), and the Association for Assessment and Accreditation of Laboratory Animal Care International.

Statistical analyses

The relationship between pSTAT3 expression and EC_{50} for erlotinib in the 4 HNSCC cell lines was analyzed using nonparametric correlation (Spearman) and 2-tailed test for comparing 2 groups. The *in vitro* comparison of pSTAT3 expression in the sensitive (T24) and the cetuximab-resistant bladder cancer cell lines (T24 PR1, T24 PR2, and T24 PR3) were analyzed using the Mann–Whitney test for comparing 2 groups. All tests were exact and 2-tailed. The *in vitro* comparison of IL-6 production in the sensitive (T24) and the cetuximab-resistant bladder cancer cell lines (T24 PR1, T24 PR2, and T24 PR3) were analyzed using the

Published OnlineFirst July 23, 2012; DOI: 10.1158/1078-0432.CCR-12-0792

Mann–Whitney test for comparing 2 groups. All tests were approximate and 2-tailed. *In vitro* comparisons of Bcl-X_L and cyclin D1 expression levels and the differences in STAT3 in HNSCC patient biopsies between treatment groups were conducted using the Mann–Whitney test for comparing 2 groups. All tests were exact and 2-tailed. For the statistical analyses of the *in vivo* experiment involving the cetuximab-resistant bladder cancer cell line T24 PR3 and the isogenic parental cell line T24 treated with STAT3 decoy and cetuximab, all comparisons were conducted on tumor volume measurements on day 20, the last day of the xenograft experiment. The 2 cell lines (parental and resistant) were compared by testing the difference between the 2 groups of mice, each bearing one cell line, with a 2-tailed Wilcoxon test. The effect of STAT3 decoy was evaluated by testing whether the inter-flank tumor volumes (STAT3 decoy on one flank, mutant control decoy on the other) differed from 0 by a 2-tailed signed-rank test. For the statistical analyses of the *in vivo* experiment involving the TKI-resistant HNSCC cell line treated with STAT3 decoy and cetuximab, tumor volumes were natural log-transformed. A mixed-effects polynomial regression model was fit to the tumor growth curves for each treatment group. Structured covariance matrices were estimated for with-mouse variation across time. A restricted maximum likelihood test was constructed to determine the appropriate choice for model parameters. A two degree of freedom test was constructed to simultaneously test the equality of the linear and quadratic regression parameters. Residuals were inspected to evaluate the adequacy of fit.

Results

Phospho-STAT3 levels and erlotinib sensitivity in HNSCC cell lines

With the goal of comparing STAT3 activation in cells that are sensitive or resistant to EGFR TKI, we treated HNSCC cell lines with varying doses of erlotinib. Two HNSCC cell lines showed relatively high EC_{50} concentrations (4.6 and 4.3 μmol/L for 686LN and Cal33, respectively) and 2 HNSCC cell lines with lower EC_{50} concentrations (1.4 and 0.364 μmol/L for OSC19 and HN5, respectively; Fig. 1A). We next assessed the levels of total STAT3 and tyrosine705 phosphorylated STAT3 (pSTAT3) in the 4 cell lines. The cells with greater EC_{50} for erlotinib (686LN and Cal33) exhibited increased pSTAT3 expression relative to the cells which were more sensitive to erlotinib and showed less pSTAT3 expression (OSC19 and HN5), with Spearman correlation coefficient (r) of 1, $P = 0.08$ (Fig. 1B). Although these results do not suggest a significant correlation but the trend indicated that STAT3 activation may be associated with intrinsic EGFR TKI resistance in HNSCC cell lines.

Increased expression of phosphotyrosine STAT3 in cetuximab-resistant cell lines

We next sought to determine whether pSTAT3 levels are increased in the setting of acquired resistance to the monoclonal antibody cetuximab. Because HNSCC cell lines are not reproducibly growth inhibited by cetuximab *in vitro* whereas HNSCC cell line xenografts are uniformly sensitive to cetuximab *in vivo*, it was not possible to determine the association between STAT3 activation and intrinsic resistance to cetuximab. Treatment of cetuximab-sensitive (T24) and cetuximab-resistant bladder cancer cell lines (T24 PR1, T24 PR2, and T24 PR3) with erlotinib showed comparable EC_{50} values (see Supplementary Fig. S1). We recently developed an *in vivo* model of acquired resistance to cetuximab using T24 bladder carcinoma cells (27). As shown in Fig. 2A and B, expression of pSTAT3 was increased from 3.2- to 3.9-fold in the cetuximab-resistant cell lines (T24 PR1, T24 PR2, and T24 PR3) compared with the isogenic parental cell line, which retains sensitivity to cetuximab. Although levels of total and/or phosphorylated EGFR and JAKs 1–3 did not differ between cetuximab-sensitive and -resistant cells, a significant increase in IL-6 secretion was found in the cetuximab-resistant bladder cancer cell lines (T24 PR1,

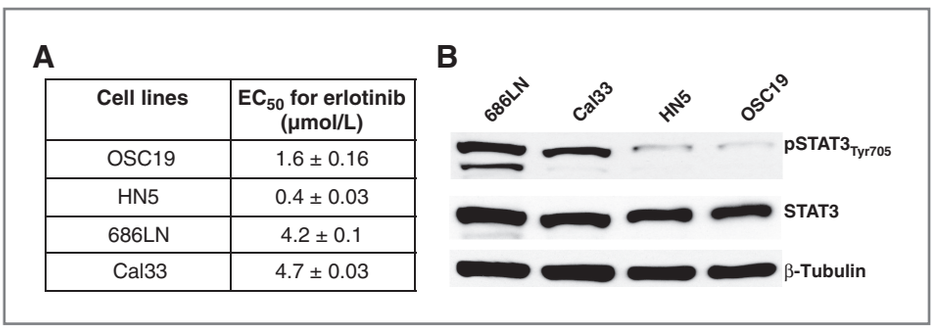

Cell lines	EC_{50} for erlotinib (μmol/L)
OSC19	1.6 ± 0.16
HN5	0.4 ± 0.03
686LN	4.2 ± 0.1
Cal33	4.7 ± 0.03

Figure 1. pSTAT3 expression levels and erlotinib sensitivity in HNSCC cell lines. A, representative HNSCC cell lines (OSC19, HN5, 686LN, and Cal33) were treated with varying concentrations of erlotinib. After 72 hours, MTT assays were conducted and EC_{50} values were calculated. The experiment was carried out 2 times with similar results. B, representative HNSCC cell lines (OSC19, HN5, 686LN, and Cal33) were seeded in 10-cm plates (1×10^6 cells), and after 24 hours, cells were harvested to obtain cell lysates. Forty micrograms of protein per lane was subjected to electrophoresis and immunoblotted for $pSTAT3_{Tyr705}$ and total STAT3. β-Tubulin was used as a loading control. The HNSCC cell lines with higher EC_{50}s for erlotinib (Cal33 and 686LN) showed higher pSTAT3 levels than in the HNSCC cell lines exhibiting lower EC_{50} values for erlotinib (OSC19 and HN5) with a Spearman correlation coefficient of 1, $P = 0.08$. The experiment was repeated 2 times with similar results.

Published OnlineFirst July 23, 2012; DOI: 10.1158/1078-0432.CCR-12-0792

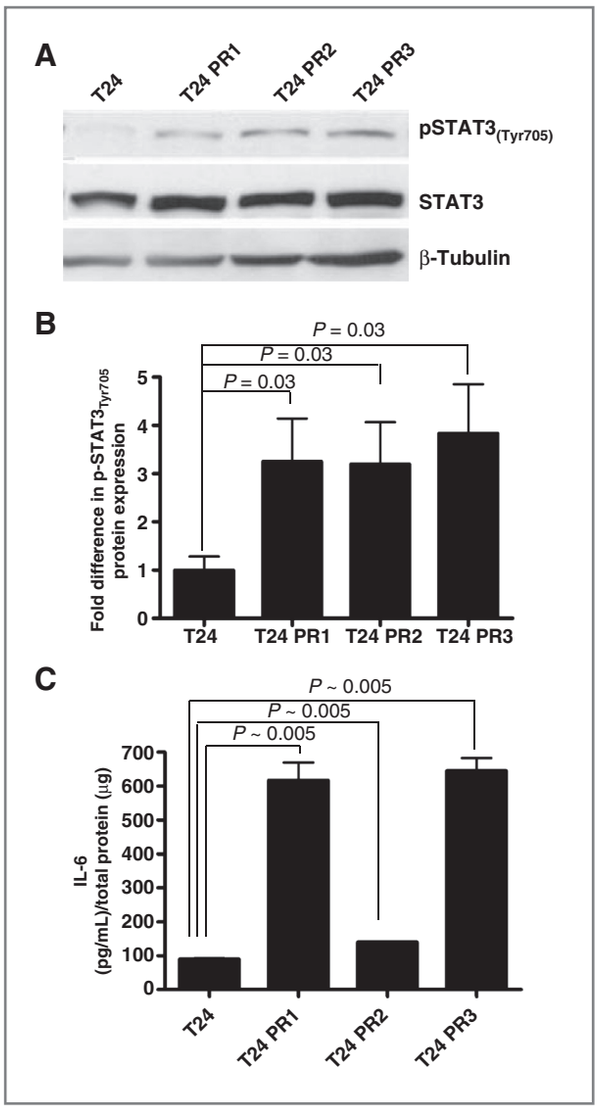

Figure 2. A, pSTAT3 protein expression is increased in cetuximab-resistant cancer cells. Cetuximab-sensitive parental T24 cells and isogenic clones showing acquired resistance to cetuximab (T24 PR1, T24 PR2, and T24 PR3) were subjected to immunoblotting for $pSTAT3_{Tyr705}$ and STAT3. β-Tubulin was used as a loading control. B, pSTAT3 expression was increased by 3.2- to 3.9-fold in the cetuximab-resistant T24 PR1, T24 PR2, and T24 PR3 cells compared with the isogenic cetuximab-sensitive T24 cells ($P = 0.03$). The experiment was repeated 4 times with similar results. C, IL-6–secreted protein levels increase in cetuximab-resistant bladder cancer cells (T24 PR1, T24 PR2, and T24 PR3, $P \sim 0.005$) compared with the sensitive counterpart (T24) as confirmed by ELISA.

T24 PR2, and T24 PR3) compared with the sensitive T24 cells (Fig. 2C; $P \sim 0.005$).

Growth of EGFR inhibitor–resistant cells is abrogated by STAT3 blockade

To determine whether targeting STAT3 can reduce the growth rate of cells showing intrinsic or acquired resistance to EGFR inhibitors, we first tested the effect of the STAT3 decoy on cell proliferation in the models of intrinsic erlotinib resistance and acquired cetuximab resistance. Cetuximab-sensitive parental T24 cells and cetuximab-resistant clones T24 PR1, T24 PR2, and T24 PR3, as well as the HNSCC cell lines showing intrinsic erlotinib resistance (or sensitivity) were treated with increasing concentrations of STAT3 decoy or a mutant control decoy that differs only by a single base pair and fails to interfere with STAT3-mediated DNA binding (18). In 72-hour treatment assays, the STAT3 decoy exhibited highly similar EC_{50} values in both the parental and cetuximab-resistant cell lines (T24: EC_{50} = 3.9 nmol/L, T24 PR1: EC_{50} = 3.6 nmol/L, T24 PR2: EC_{50} = 2.8 nmol/L, and T24 PR3: EC_{50} = 4.7 nmol/L; Fig. 3). In the erlotinib-sensitive and -resistant HNSCC cell lines, the STAT3 decoy exhibited comparable EC_{50} values, ranging between 5 and 11 nmol/L. Although these cells expressed different levels of pSTAT3, they exhibited similar sensitivity to the STAT3 decoy. Similar findings were observed with the preclinical JAK/STAT inhibitor JSI-124 (data not shown). These findings indicate that STAT3 targeting decreases cell proliferation in cancer cells that exhibit either intrinsic or acquired resistance to EGFR inhibitors.

STAT3 decoy downmodulates STAT3 target gene expression in EGFR inhibitor–resistant cells

Abrogation of target gene expression is a biochemical indication that the STAT3 decoy is blocking STAT3-

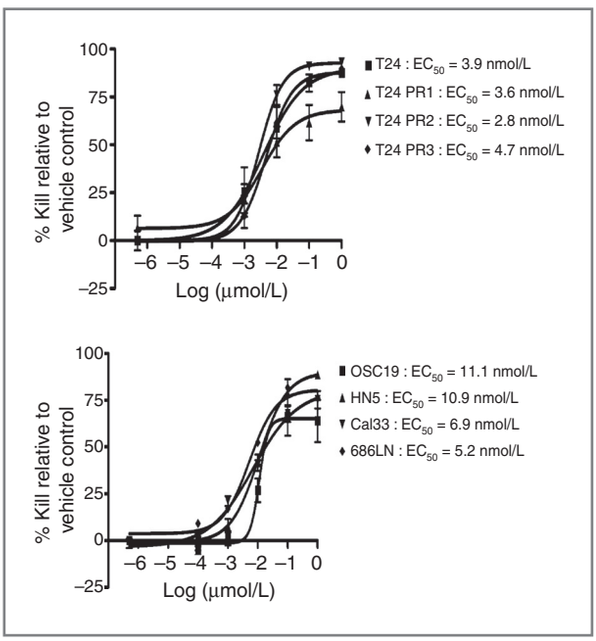

Figure 3. Targeting STAT3 inhibits proliferation of cancer cell lines with intrinsic or acquired resistance to EGFR inhibitors. Erlotinib-sensitive (OSC19 and HN5) and erlotinib-resistant (686LN and Cal33 cells) HNSCC cell lines and cetuximab-sensitive (T24) and cetuximab-resistant cancer cells (T24 PR1, T24 PR2, and T24 PR3) were treated with a range of concentrations of the STAT3 decoy. After 72 hours, MTT assays were conducted and EC_{50} values were calculated. The experiment was carried out 3 times with similar results. Each data point in the curve represents mean ± SD.

Published OnlineFirst July 23, 2012; DOI: 10.1158/1078-0432.CCR-12-0792

mediated signaling. To determine the effect of the STAT3 decoy on the expression of STAT3 target genes in EGFR inhibitor–resistant models, cells were treated with EC_{50} concentrations of STAT3 decoy, followed by immunoblotting for the STAT3 target genes, cyclin D1 and Bcl-X_L. β-Tubulin was assessed as a loading control. In the parental cetuximab-sensitive and the -resistant cells, treatment with STAT3 decoy resulted in a significant decrease in expression of Bcl-X_L and cyclin D1 in T24 ($P = 0.057$ and 0.029, respectively), T24 PR1 ($P = 0.029$ and 0.029, respectively), T24 PR2 ($P = 0.029$ and 0.029, respectively), and T24 PR3 ($P = 0.029$ and 0.029, respectively) cells, when compared with treatment with vehicle (Fig. 4A–D, respectively). Similarly, treatment with STAT3 decoy led to downmodulation of cyclin D1 and Bcl-X_L in both the erlotinib-sensitive (Supplementary Fig. S2A and S2B) and -resistant HNSCC cell lines (Supplementary Fig. S2C and S2D). In the erlotinib-sensitive and -resistant HNSCC cells, treatment with the STAT3 decoy led to a significant decrease in expression of Bcl-X_L and cyclin D1 in OSC19 ($P = 0.029$ and 0.029, respectively), HN5 ($P = 0.057$ and 0.029, respectively), Cal33 ($P = 0.057$ and 0.029, respectively), and 686LN ($P = 0.029$ and 0.029, respectively) cells, in comparison with treatment with vehicle (Supplementary Fig. S2A–S2D, respectively)

Targeting STAT3 augments the *in vivo* antitumor effects of cetuximab in both cetuximab-sensitive and cetuximab-resistant models

Despite widespread EGFR expression in most epithelial malignancies, cetuximab is only effective in a subset of patients with cancer. Because pSTAT3 levels are elevated in HNSCC cells (Fig. 2 was done *in vitro*, not with xenograft tumors) showing acquired cetuximab resistance, we assessed the antitumor effects of the STAT3 decoy in combination with cetuximab in cetuximab-sensitive (T24) and cetuximab-resistant xenografts (T24 PR3). Mice bearing xenograft tumors (9 mice per group) were treated with daily intratumoral injections (50 μg) of the STAT3 decoy (or the mutant control decoy) in combination with intraperitoneal cetuximab (1 mg), 3 times a week. As shown in Fig. 5A, treatment with the STAT3 decoy plus cetuximab showed a small but significant growth inhibition of tumors generated from the cetuximab-sensitive parental cell line (T24) when compared with treatment with STAT3 mutant control decoy plus cetuximab ($P = 0.0078$). Profoundly, treatment of cetuximab-resistant tumors with STAT3 decoy in combination with cetuximab resulted in substantial and significant tumor growth inhibition in comparison with treatment with STAT3 mutant control decoy and cetuximab ($P = 0.0078$). At the end of treatment, tumors were harvested and assessed for expression of proteins encoded by STAT3 target genes. Cetuximab-sensitive tumors treated with STAT3 decoy plus cetuximab showed a decrease in Bcl-X_L ($P = 0.03$) and cyclin D1 ($P = 0.05$) expression when compared with treatment with STAT3 mutant control decoy plus cetuximab. Similarly, cetuximab-resistant tumors treated with STAT3 decoy plus cetuximab showed in a decrease in Bcl-X_L ($P = 0.0071$) and cyclin D1 ($P = 0.05$) expression when compared with treatment with STAT3 mutant control decoy plus cetuximab (Fig. 5B and C). These results indicate that inhibition of STAT3 may be an effective therapeutic strategy in the setting of cetuximab resistance.

STAT3 decoy inhibits tumor growth *in vivo* of TKI-resistant HNSCC xenografts

The effect of STAT3 decoy was also assessed in combination with cetuximab in TKI-resistant xenograft tumors generated from the HNSCC cell line 686LN. 686LN (1×10^6 cells) were inoculated subcutaneously in 10 athymic nude mice into the right and left flank. After 8 days, when the tumors were clearly palpable, mice were treated with daily intratumoral injections of the STAT3 decoy/STAT3 mutant (50 μg). Cetuximab was administered at a dose of 0.2 mg/mouse, 2 times a week intraperitoneally. Tumors were measured 3 times per week. At the end of day 20, TKI-resistant HNSCC xenografts treated with STAT3 decoy + cetuximab showed a significant decrease in tumor volume when compared with the xenografts treated with STAT3 mutant control + cetuximab ($P < 0.0001$; Supplementary Fig. S3).

Human HNSCC tumors that recur following cetuximab treatment demonstrate increased p-STAT3

Cetuximab was FDA-approved for the treatment of HNSCC in 2006. To date, no study has systematically characterized HNSCC tumors that persist or develop following treatment with cetuximab. To begin to understand the mechanisms of clinical resistance to cetuximab, we created a TMA containing HNSCC tumor samples before and/or following treatment with cetuximab-containing regimens at the University of Pittsburgh, as described previously (28). Immunohistochemical staining of the TMA with anti-pSTAT3 was conducted. Expression of pSTAT3 expression in tumor samples following disease progression after cetuximab treatment was elevated compared with levels in tumors biopsies obtained before cetuximab administration (Fig. 6A). Figure 6B shows representative pSTAT3 IHC from 3 tumors before cetuximab treatment (top) and 3 tumors following cetuximab treatment (bottom). These findings from a small and heterogeneous HNSCC patient cohort suggest that pSTAT3 may represent a potential therapeutic target to improve responses to EGFR-targeted therapy.

Discussion

Persistent activation of STAT3 has been implicated in conferring resistance to conventional therapies in some malignancies. Elevated levels of STAT3 have been reported in several drug-resistant cancer cells where inactivation of STAT3 reversed the multidrug-resistant phenotype (29).

Several strategies have been developed to target the STAT3 pathway in settings of intrinsic resistance to chemotherapy and radiation in preclinical cancer models. In an *in vivo* model of NSCLC, inhibition of STAT3 using the STAT3 pathway inhibitor cucurbitacin I (JSI-124), a triterpenoid

Published OnlineFirst July 23, 2012; DOI: 10.1158/1078-0432.CCR-12-0792

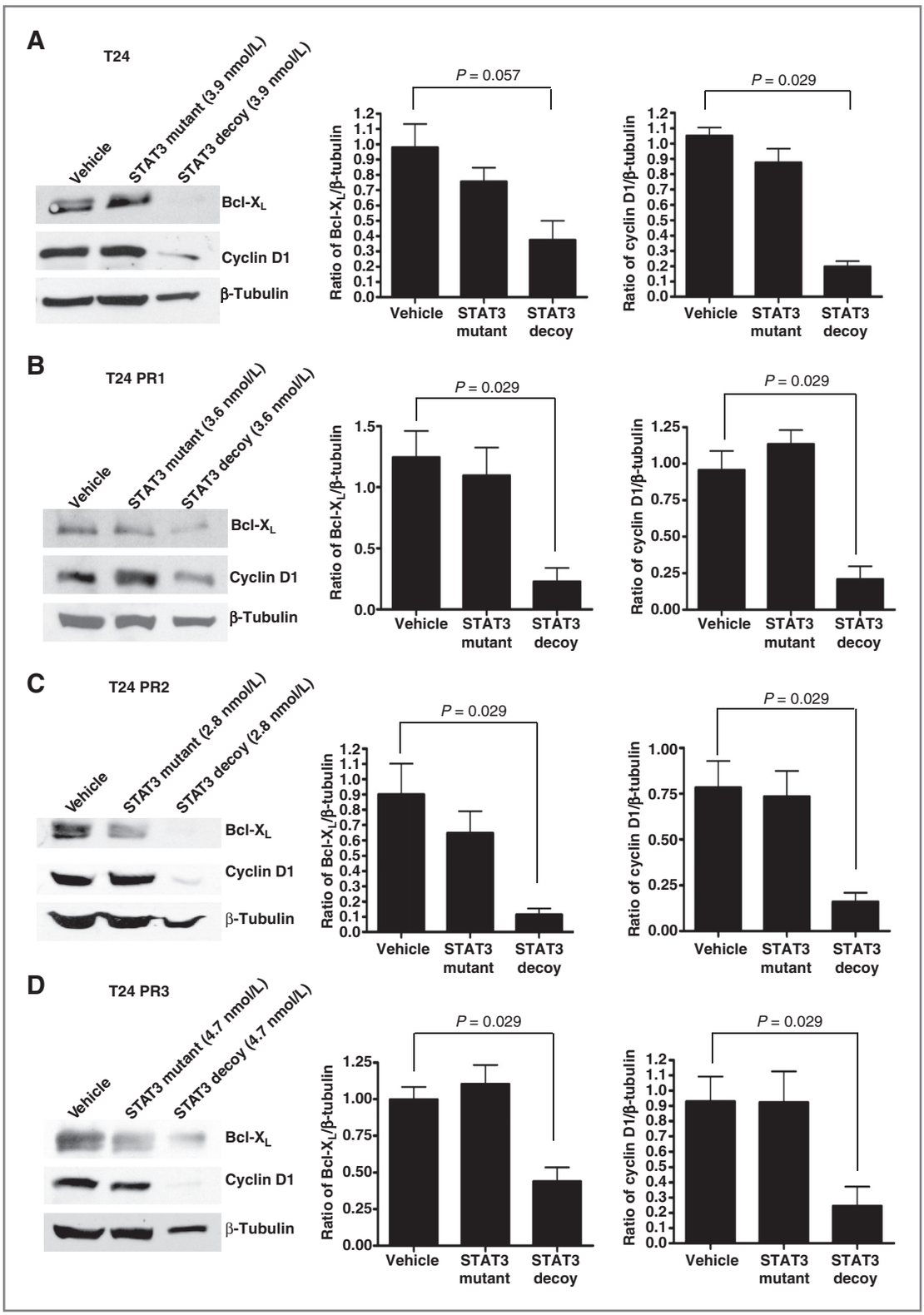

Figure 4. A–D, decreased STAT3 target gene expression in cetuximab-sensitive (or resistant) cells following treatment with the STAT3 decoy. Cetuximab-sensitive (T24) and cetuximab-resistant (T24 PR1, T24 PR2, and T24 PR3) bladder cancer cells were treated with STAT3 decoy at EC_{50} concentrations. As controls, cells were treated with vehicle alone or the mutant control STAT3 decoy. After 72 hours, cells were harvested and proteins (40 μg/lane) were subjected to electrophoresis and immunoblotted for cyclin D1 or Bcl-X_L. β-Tubulin was used as a loading control. The experiment was repeated 4 times with similar results.

Published OnlineFirst July 23, 2012; DOI: 10.1158/1078-0432.CCR-12-0792

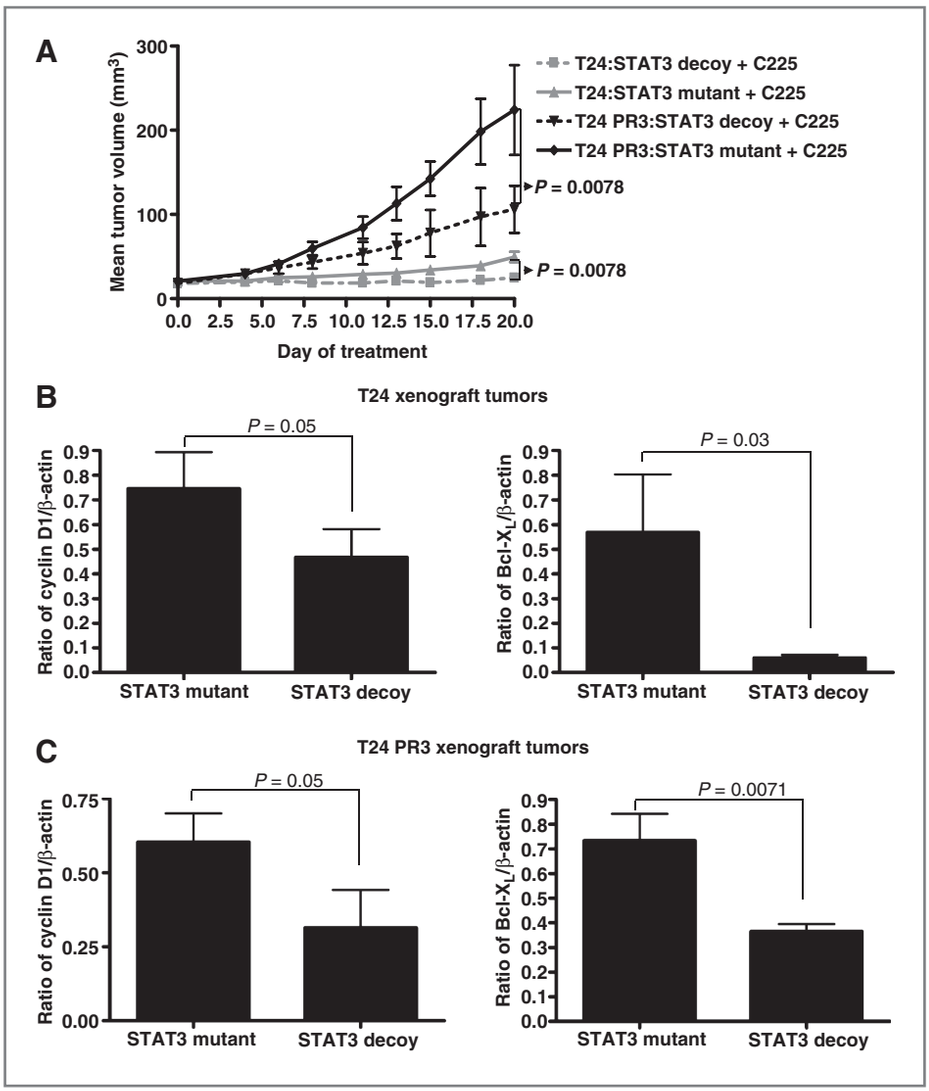

Figure 5. STAT3 decoy inhibits *in vivo* growth of cetuximab-sensitive and -resistant xenograft tumors while downregulating target gene expression. A, T24 and T24 PR3 cells (2×10^6 cells) were inoculated subcutaneously in 9 athymic nude mice per cell line in the right and left flanks. After 4 days, when the tumors were clearly palpable, the tumor on the right flank was treated with daily injections of the STAT3 decoy (50 μg) and the tumor on the left flank was treated with the STAT3 mutant control decoy (50 μg). Mice were also given cetuximab at a dose of 1 mg/mouse, 3 times a week intraperitoneally. Tumors were measured 3 times per week. At the end of day 20, the cetuximab-sensitive parental xenografts (T24) treated with STAT3 decoy + cetuximab showed a significant decrease in tumor volume compared with the T24 xenografts treated with STAT3 mutant control decoy + cetuximab ($P = 0.0078$). In addition, the cetuximab-resistant T24 PR3 xenografts treated with STAT3 decoy + cetuximab showed a significant decrease in tumor volume compared with the T24 PR3 xenografts treated with STAT3 mutant control decoy + cetuximab ($P = 0.0078$). B, STAT3 decoy downmodulates STAT3 target gene expression in cetuximab-resistant xenograft tumors. Mice from the experiment described in A were sacrificed after 20 days and tumors were harvested for analysis of STAT3 target gene expression. In the cetuximab-sensitive parental xenografts (T24) treated with STAT3 decoy + cetuximab, decreases in Bcl-X_L ($P = 0.03$) and cyclin D1 ($P = 0.05$) were observed when compared with tumors treated with STAT3 mutant control decoy + cetuximab (top). Similarly, decreases in Bcl-X_L ($P = 0.0071$) and cyclin D1 ($P = 0.05$) expressions were observed in the cetuximab-resistant tumors (T24 PR3) treated with STAT3 decoy + cetuximab compared with the tumors treated with STAT3 mutant control decoy + cetuximab (bottom).

derivative, was able to overcome resistance to chemotherapy or radiotherapy (30). Inhibition of STAT3 reportedly sensitized glioma cells to temozolomide, an alkylator-based chemotherapy (31). In bladder cancer, aberrant STAT3 activation has been associated with chemoresistance, where subsequent inhibition of STAT3 activation by STAT3 siRNA or treatment with the JAK2 inhibitor AG-490, increased the sensitivity of the cells to chemotherapeutic agents (32). Others have reported that AG-490 treatment restores chemosensitivity in drug-resistant hematopoietic tumor cells (33). Using *in vivo* HNSCC models, cucurbitacin I treatment enhanced the inhibitory effects of ionizing radiation and abrogated radioresistance (34).

Several studies have shown that acquired therapeutic resistance is associated with enhanced activation of the STAT3 where inhibiting the STAT3 pathway can restore

Published OnlineFirst July 23, 2012; DOI: 10.1158/1078-0432.CCR-12-0792

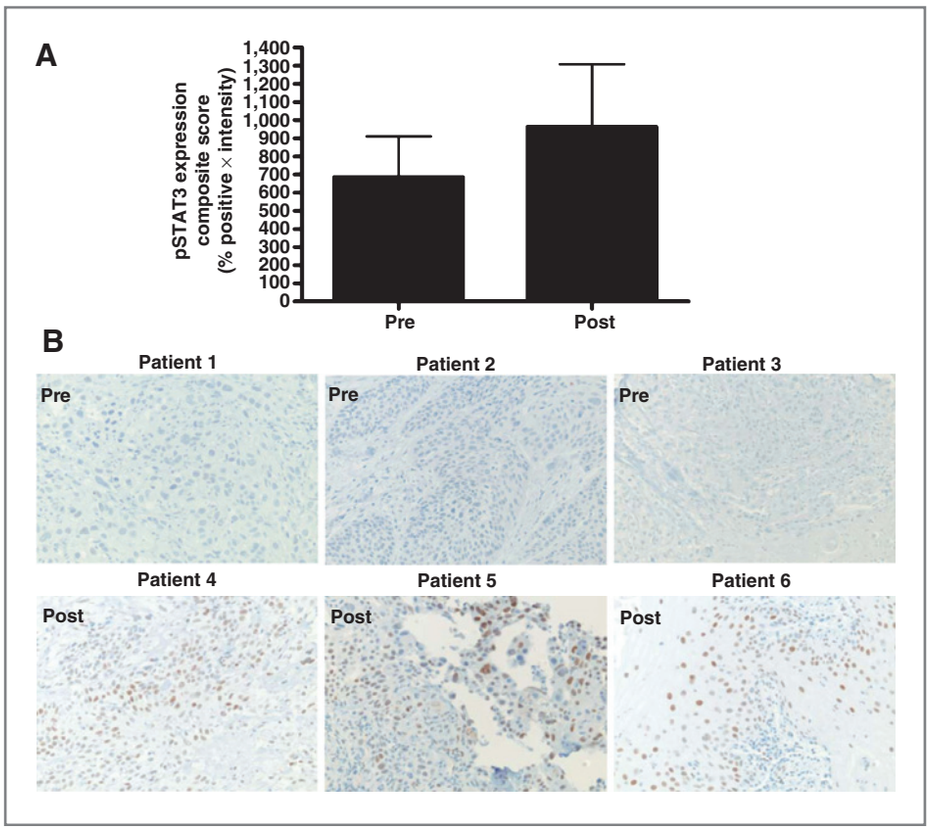

Figure 6. Human HNSCC tumors from cetuximab-treated patients exhibit increased pSTAT3 expression compared with pretreatment tumors. A, cumulative results from 7 tumors before cetuximab treatment and 15 tumors follow cetuximab treatment from TMA stained with pSTAT3 antibody. The average composite score (intensity of staining × the percentage of tumor cells that stained positively) of pre- and post–cetuximab-treated tumors are represented. B, representative pSTAT3 IHC from 3 tumors before cetuximab treatment (top) and 3 tumors following cetuximab treatment (bottom).

drug sensitivity (35, 36). In gastric cancer, the STAT3 pathway has been shown to be involved in acquired drug resistance and inhibition of STAT3 by the STAT3-SH2 antagonist, 5,15-diphenylporphyrin (DPP), sensitized resistant cells to chemotherapy (37). In ovarian cancer models, acquisition of drug resistance was correlated with STAT3 activation both *in vitro* where resistance to paclitaxel has been associated with increased expression of pSTAT3 as well as in a human tumor tissue array, where recurrent or metastatic lesions showed increased pSTAT3 expression compared with levels in the primary tumor (38). They further showed that *in vitro* inhibition of the STAT3 pathway using the triterpenoid CDDO-Me reverses paclitaxel resistance in ovarian cancer cell lines (39). In breast cancer, tamoxifen resistance was associated with activation of STAT3, supporting the use of STAT3 inhibitors to overcome acquired tamoxifen resistance (40). Both constitutive and inducible STAT3 activation has been reported in acute myeloid leukemias (AML) and AML cell lines where the use of the small-molecule probe C188 that targets the phosphotyrosine (pY) peptide binding site within the STAT3 SH2 domain can sensitize the drug-resistant tumor cells (41).

Several studies have implicated STAT3 activation in EGFR resistance. In hepatocellular carcinoma, cetuximab resistance was mediated via STAT3 activation, and combination therapy using both inhibitors of EGFR and STAT3 *in vitro* enhanced growth inhibition (42). In NSCLCs, STAT3 activation conferred resistance to NSCLC against gefitinib, which was restored upon suppression of STAT3 activity, suggesting that in patients with NSCLCs who are insensitive to EGFR inhibitors, STAT3 targeting maybe considered as an alternative therapy (43). In a pilot study where activated signaling molecules were evaluated in patients with NSCLCs who received gefitinib before surgical resection of tumor, pSTAT3 levels were elevated in the surgically resected tumor tissue implicating STAT3 as a potential candidate in mediating primary resistance (17). In high-grade glioma, elevated levels of pSTAT3 has been linked to chemoresistance and blockade of STAT3 signaling sensitized the glioma cells to chemotherapy, thus providing a rationale for use of targeted therapies against STAT3 (16). In the present study, we identified STAT3 activation and increased IL-6 production in preclinical cancer models of intrinsic and acquired resistance to EGFR inhibitors. Our results show that targeting STAT3 using the STAT3 decoy in cetuximab- or TKI-resistant cells sensitizes the cells to EGFR inhibitor treatment *in vitro* and *in vivo*. The STAT3 decoy has also been tested in leukemia where inhibition of hyperactivated STAT3 in adriamycin-resistant K562/A02 leukemia cells by the STAT3 decoy increased the sensitivity of the cells to adriamycin (29). Further investigation showed activation of pSTAT3 in human HNSCC tumors who recurred following cetuximab treatment, suggesting that STAT3 activation is associated with cetuximab resistance. These cumulative findings suggest that strategies that inhibit STAT3 may abrogate therapeutic resistance to EGFR inhibitors.

Published OnlineFirst July 23, 2012; DOI: 10.1158/1078-0432.CCR-12-0792

Disclosure of Potential Conflicts of Interest

No potential conflicts of interest were disclosed.

Authors' Contributions

Conception and design: M. Sen, S.M. Thomas, D.E. Johnson, J.R. Grandis
Development of methodology: S.M. Thomas
Acquisition of data (provided animals, acquired and managed patients, provided facilities, etc.): S.M. Thomas, J. Maxwell
Analysis and interpretation of data (e.g., statistical analysis, biostatistics, computational analysis): M. Panahandeh, S.M. Thomas, L. Wang, W.E. Gooding, D.E. Johnson, J.R. Grandis
Writing, review, and/or revision of the manuscript: M. Sen, D.E. Johnson, J.R. Grandis
Administrative, technical, or material support (i.e., reporting or organizing data, constructing databases): M. Panahandeh, C. Li, J. Maxwell
Conducted experiments, analyzed and interpreted data: M. Sen

Acknowledgments

The authors thank Kelly M. Quesnelle, University of Pittsburgh, for providing the cetuximab-resistant bladder cancer cell models.

Grant Support

This work was supported by NIH grants R01CA098372 and P50CA097190 as well as the American Cancer Society to J.R. Grandis, and NIH grant R01CA137260 to D.E. Johnson.

The costs of publication of this article were defrayed in part by the payment of page charges. This article must therefore be hereby marked *advertisement* in accordance with 18 U.S.C. Section 1734 solely to indicate this fact.

Received March 6, 2012; revised June 8, 2012; accepted July 3, 2012; published OnlineFirst July 23, 2012.

References

1. Camp ER, Summy J, Bauer TW, Liu W, Gallick GE, Ellis LM. Molecular mechanisms of resistance to therapies targeting the epidermal growth factor receptor. Clin Cancer Res 2005;11:397–405.
2. Ciardiello F, Tortora G. EGFR antagonists in cancer treatment. N Engl J Med 2008;358:1160–74.
3. Harandi A, Zaidi AS, Stocker AM, Laber DA. Clinical efficacy and toxicity of anti-EGFR therapy in common cancers. J Oncol 2009;2009:567486.
4. Yamatodani T, Ekblad L, Kjellen E, Johnsson A, Mineta H, Wennerberg J. Epidermal growth factor receptor status and persistent activation of Akt and p44/42 MAPK pathways correlate with the effect of cetuximab in head and neck and colon cancer cell lines. J Cancer Res Clin Oncol 2009;135:395–402.
5. Schilder RJ, Sill MW, Chen X, Darcy KM, Decesare SL, Lewandowski G, et al. Phase II study of gefitinib in patients with relapsed or persistent ovarian or primary peritoneal carcinoma and evaluation of epidermal growth factor receptor mutations and immunohistochemical expression: a Gynecologic Oncology Group Study. Clin Cancer Res 2005;11:5539–48.
6. Small EJ, Fontana J, Tannir N, DiPaola RS, Wilding G, Rubin M, et al. A phase II trial of gefitinib in patients with non-metastatic hormone-refractory prostate cancer. BJU Int 2007;100:765–9.
7. Thatcher N, Chang A, Parikh P, Rodrigues Pereira J, Ciuleanu T, von Pawel J, et al. Gefitinib plus best supportive care in previously treated patients with refractory advanced non-small-cell lung cancer: results from a randomised, placebo-controlled, multicentre study (Iressa Survival Evaluation in Lung Cancer). Lancet 2005;366:1527–37.
8. Goodin S. Erlotinib: optimizing therapy with predictors of response? Clin Cancer Res 2006;12:2961–3.
9. Yao Z, Fenoglio S, Gao DC, Camiolo M, Stiles B, Lindsted T, et al. TGF-beta IL-6 axis mediates selective and adaptive mechanisms of resistance to molecular targeted therapy in lung cancer. Proc Natl Acad Sci U S A 2010;107:15535–40.
10. Tabernero J. The role of VEGF and EGFR inhibition: implications for combining anti-VEGF and anti-EGFR agents. Mol Cancer Res 2007;5:203–20.
11. Morgillo F, Cantile F, Fasano M, Troiani T, Martinelli E, Ciardiello F. Resistance mechanisms of tumour cells to EGFR inhibitors. Clin Transl Oncol 2009;11:270–5.
12. Kijima T, Niwa H, Steinman RA, Drenning SD, Gooding WE, Wentzel AL, et al. STAT3 activation abrogates growth factor dependence and contributes to head and neck squamous cell carcinoma tumor growth *in vivo*. Cell Growth Differ 2002;13:355–62.
13. Kim HS, Park YH, Lee J, Ahn JS, Kim J, Shim YM, et al. Clinical impact of phosphorylated signal transducer and activator of transcription 3, epidermal growth factor receptor, p53, and vascular endothelial growth factor receptor 1 expression in resected adenocarcinoma of lung by using tissue microarray. Cancer 2010;116:676–85.
14. Schindler C, Darnell JE Jr. Transcriptional responses to polypeptide ligands: the JAK-STAT pathway. Annu Rev Biochem 1995;64:621–51.
15. Cao X, Tay A, Guy GR, Tan YH. Activation and association of Stat3 with Src in v-Src-transformed cell lines. Mol Cell Biol 1996;16:1595–603.
16. Lo HW, Cao X, Zhu H, Ali-Osman F. Constitutively activated STAT3 frequently coexpresses with epidermal growth factor receptor in high-grade gliomas and targeting STAT3 sensitizes them to Iressa and alkylators. Clin Cancer Res 2008;14:6042–54.
17. Haura EB, Sommers E, Song L, Chiappori A, Becker A. A pilot study of preoperative gefitinib for early-stage lung cancer to assess intratumor drug concentration and pathways mediating primary resistance. J Thorac Oncol 2010;5:1806–14.
18. Leong PL, Andrews GA, Johnson DE, Dyer KF, Xi S, Mai JC, et al. Targeted inhibition of Stat3 with a decoy oligonucleotide abrogates head and neck cancer cell growth. Proc Natl Acad Sci U S A 2003;100:4138–43.
19. Xi S, Gooding WE, Grandis JR. *In vivo* antitumor efficacy of STAT3 blockade using a transcription factor decoy approach: implications for cancer therapy. Oncogene 2005;24:970–9.
20. Zhang X, Zhang J, Wei H, Tian Z. STAT3-decoy oligodeoxynucleotide inhibits the growth of human lung cancer via down-regulating its target genes. Oncol Rep 2007;17:1377–82.
21. Sun Z, Yao Z, Liu S, Tang H, Yan X. An oligonucleotide decoy for Stat3 activates the immune response of macrophages to breast cancer. Immunobiology 2006;211:199–209.
22. Shen J, Li R, Li G. Inhibitory effects of decoy-ODN targeting activated STAT3 on human glioma growth *in vivo*. In Vivo 2009;23:237–43.
23. Pedranzini L, Leitch A, Bromberg J. Stat3 is required for the development of skin cancer. J Clin Invest 2004;114:619–22.
24. Sun X, Zhang J, Wang L, Tian Z. Growth inhibition of human hepatocellular carcinoma cells by blocking STAT3 activation with decoy-ODN. Cancer Lett 2008;262:201–13.
25. Souissi I, Najjar I, Ah-Koon L, Schischmanoff PO, Lesage D, Le Coquil S, et al. A STAT3-decoy oligonucleotide induces cell death in a human colorectal carcinoma cell line by blocking nuclear transfer of STAT3 and STAT3-bound NF-kappaB. BMC Cell Biol 2011;12:14.
26. Boehm AL, Sen M, Seethala R, Gooding WE, Freilino M, Wong SM, et al. Combined targeting of epidermal growth factor receptor, signal transducer and activator of transcription-3, and Bcl-X(L) enhances antitumor effects in squamous cell carcinoma of the head and neck. Mol Pharmacol 2008;73:1632–42.
27. Quesnelle KM, Grandis JR. Dual kinase inhibition of EGFR and HER2 overcomes resistance to cetuximab in a novel *in vivo* model of acquired cetuximab resistance. Clin Cancer Res 2011;17:5935–44.
28. Bhola NE, Thomas SM, Freilino M, Joyce S, Sahu A, Maxwell J, et al. Targeting GPCR-mediated p70S6K activity may improve head and neck cancer response to cetuximab. Clin Cancer Res 2011;17:4996–5004.
29. Zhang X, Xiao W, Wang L, Tian Z, Zhang J. Deactivation of signal transducer and activator of transcription 3 reverses chemotherapeutics resistance of leukemia cells via down-regulating P-gp. PLoS One 2011;6:e20965.

Published OnlineFirst July 23, 2012; DOI: 10.1158/1078-0432.CCR-12-0792

30. Hsu HS, Huang PI, Chang YL, Tzao C, Chen YW, Shih HC, et al. Cucurbitacin I inhibits tumorigenic ability and enhances radiochemosensitivity in nonsmall cell lung cancer-derived CD133-positive cells. Cancer 2011;117:2970–85.
31. Wang Y, Chen L, Bao Z, Li S, You G, Yan W, et al. Inhibition of STAT3 reverses alkylator resistance through modulation of the AKT and beta-catenin signaling pathways. Oncol Rep 2011;26:1173–80.
32. Chen RJ, Ho YS, Guo HR, Wang YJ. Long-term nicotine exposure-induced chemoresistance is mediated by activation of Stat3 and downregulation of ERK1/2 via nAChR and beta-adrenoceptors in human bladder cancer cells. Toxicol Sci 2010;115:118–30.
33. Alas S, Bonavida B. Inhibition of constitutive STAT3 activity sensitizes resistant non-Hodgkin's lymphoma and multiple myeloma to chemotherapeutic drug-mediated apoptosis. Clin Cancer Res 2003;9:316–26.
34. Chen YW, Chen KH, Huang PI, Chen YC, Chiou GY, Lo WL, et al. Cucurbitacin I suppressed stem-like property and enhanced radiation-induced apoptosis in head and neck squamous carcinoma–derived CD44(+)ALDH1(+) cells. Mol Cancer Ther 2010;9:2879–92.
35. Bewry NN, Nair RR, Emmons MF, Boulware D, Pinilla-Ibarz J, Hazlehurst LA. Stat3 contributes to resistance toward BCR-ABL inhibitors in a bone marrow microenvironment model of drug resistance. Mol Cancer Ther 2008;7:3169–75.
36. Zhou J, Bi C, Janakakumara JV, Liu SC, Chng WJ, Tay KG, et al. Enhanced activation of STAT pathways and overexpression of survivin confer resistance to FLT3 inhibitors and could be therapeutic targets in AML. Blood 2009;113:4052–62.
37. Yang J, Huang J, Dasgupta M, Sears N, Miyagi M, Wang B, et al. Reversible methylation of promoter-bound STAT3 by histone-modifying enzymes. Proc Natl Acad Sci U S A 2010;107:21499–504.
38. Duan Z, Foster R, Bell DA, Mahoney J, Wolak K, Vaidya A, et al. Signal transducers and activators of transcription 3 pathway activation in drug-resistant ovarian cancer. Clin Cancer Res 2006;12:5055–63.
39. Duan Z, Ames RY, Ryan M, Hornicek FJ, Mankin H, Seiden MV. CDDO-Me, a synthetic triterpenoid, inhibits expression of IL-6 and Stat3 phosphorylation in multi-drug resistant ovarian cancer cells. Cancer Chemother Pharmacol 2009;63:681–9.
40. Ishii Y, Waxman S, Germain D. Tamoxifen stimulates the growth of cyclin D1-overexpressing breast cancer cells by promoting the activation of signal transducer and activator of transcription 3. Cancer Res 2008;68:852–60.
41. Redell MS, Ruiz MJ, Alonzo TA, Gerbing RB, Tweardy DJ. Stat3 signaling in acute myeloid leukemia: ligand-dependent and -independent activation and induction of apoptosis by a novel small-molecule Stat3 inhibitor. Blood 2011;117:5701–9.
42. Chen W, Shen X, Xia X, Xu G, Ma T, Bai X, et al. NSC 74859-mediated inhibition of STAT3 enhances the anti-proliferative activity of cetuximab in hepatocellular carcinoma. Liver Int 2012;32:70–7.
43. Chiu HC, Chou DL, Huang CT, Lin WH, Lien TW, Yen KJ, et al. Suppression of Stat3 activity sensitizes gefitinib-resistant non small cell lung cancer cells. Biochem Pharmacol 2011;81:1263–70.

Published OnlineFirst July 23, 2012; DOI: 10.1158/1078-0432.CCR-12-0792

Clinical Cancer Research

Targeting Stat3 Abrogates EGFR Inhibitor Resistance in Cancer

Malabika Sen, Sonali Joyce, Mary Panahandeh, et al.

Clin Cancer Res 2012;18:4986-4996. Published OnlineFirst July 23, 2012.